Estimating tissue iron burden: current status and future prospects

John C. Wood

Division of Cardiology, Children's Hospital Los Angeles, Los Angeles, CA, USA

Summary

Iron overload is becoming an increasing problem as haemoglobinopathy patients gain greater access to good medical care and as therapies for myelodysplastic syndromes improve. Therapeutic options for iron chelation therapy have increased and many patients now receive combination therapies. However, optimal utilization of iron chelation therapy requires knowledge not only of the total body iron burden but the relative iron distribution among the different organs. The physiological basis for extrahepatic iron deposition is presented in order to help identify patients at highest risk for cardiac and endocrine complications. This manuscript reviews the current state of the art for monitoring global iron overload status as well as its compartmentalization. Plasma markers, computerized tomography, liver biopsy, magnetic susceptibility devices and magnetic resonance imaging (MRI) techniques are all discussed but MRI has come to dominate clinical practice. The potential impact of recent pancreatic and pituitary MRI studies on clinical practice are discussed as well as other works-in-progress. Clinical protocols are derived from experience in haemoglobinopathies but may provide useful guiding principles for other iron overload disorders, such as myelodysplastic syndromes.

Keywords: iron overload, iron, thalassaemia, sickle cell anaemia, imaging.

Rationale

Despite the scarcity of bioavailable iron in our environment and the high prevalence of iron deficiency in the developing world, iron overload syndromes are surprisingly common. Iron overload can occur from hyperabsorption or from transfusion therapy. Iron hyperabsorption results from genetic errors in iron homeostasis, liver damage, or through increased erythropoetic drive (thalassaemia intermedia syndromes). Alternatively, transfusional iron overload is an iatrogenic process. Prevention of one disease, for example, stroke in sickle cell disease (SCD) patients, creates another, more insidious, disease.

Treatment of iron overload depends on the ability to support erythropoiesis. Patients with effective erythropoiesis can undergo therapeutic phlebotomy, a process that is safe and effective, although inconvenient (Adams & Barton, 2007). In fact, the National Institutes of Health-sponsored TWiTCH [Transcranial Doppler (TCD) With Transfusions Changing to Hydroxyurea] trial (NCT01425307, ClinicalTrials.gov) is comparing hydroxycarbamide (also termed hydroxyurea) therapy with phlebotomy as an alternative therapy to chronic transfusions and iron chelation in SCD patients with abnormal TCD velocities.

However, most iron overload patients with chronic anaemia have insufficient effective erythropoiesis to support phlebotomy. In these patients, lifelong iron chelation is necessary. Labile iron is quite dangerous, thus iron chelators require high chemical affinity and specificity to prevent oxidative damage. But iron is also vital to many biological processes, making overchelation dangerous. Thus monitoring iron chelation is imperative. Several factors make this difficult. First, the bioavailability of iron chelators is highly patient specific (Cohen *et al*, 2008). Secondly, iron chelation treatments are onerous, making compliance quite variable, particularly in adolescence. Thirdly, serum markers of iron overload are unreliable (Brittenham *et al*, 1993; Puliyel *et al*, 2014). Fortunately, there has been an explosion of new imaging methodologies that have changed how iron overload patients are managed (Anderson *et al*, 2001; St Pierre *et al*, 2005; Wood *et al*, 2005a; Noetzli *et al*, 2012a). This review paper discusses these techniques as well as some of the insights into disease pathophysiology that they have provided.

Review of iron regulation

Although a formal review of the proteins and signalling mechanisms involved in somatic iron regulation is beyond the scope of this review (for more comprehensive discussion, see Ganz, 2007), some understanding is useful to place iron monitoring in proper context. Total body iron balance is

Correspondence: John C. Wood, Division of Cardiology, Children's Hospital Los Angeles, MS#34, 4650 Sunset Blvd, Los Angeles, CA 90027, USA.
E-mail: jwood@chla.usc.edu

doi: 10.1111/bjh.13374

regulated by an endocrine process (Fig 1, left), while individual cells regulate iron homeostasis via molecular signalling (Fig 1, right). Iron enters the body either through the gut or through blood transfusions; transfusional iron is mobilized from haemoglobin by macrophage scavenging of senescent red blood cells. Labile iron is exported from either source to the blood stream through a unique iron transporter, known as ferroportin. In the blood stream, iron is rapidly oxidized and transported to tissues through the carrier protein, transferrin. Most transferrin-bound iron is utilized by the bone marrow for erythropoiesis. The liver also has high transferrin-bound iron uptake, serving as the primary iron reserve. Under normal iron conditions, apotransferrin (transferrin without bound iron) exists in excess, with only 25% of the binding sites carrying iron to the bone marrow, liver, and other tissues. With iron overload, transferrin saturation increases and may even reach 100%. Elevated transferrin saturation is detected by the liver, which secretes a counter-regulatory hormone called hepcidin. Hepcidin binds to ferroportin, causing its internalization and degradation, immediately reducing the influx of iron into the vascular space from the gut and reticuloendothelial system. Ferroportin internalization also secondarily triggers a cascade of events that downregulates iron absorption. Through this process, humans and other animals are protected against swings in dietary iron concentration.

However, hepcidin release is modulated by more than just transferrin saturation. Increased liver iron stores promote hepcidin secretion through BMP6-SMAD pathways, independent of transferrin saturation (Corradini *et al*, 2011). With increased erythropoiesis, red cell precursors release several factors that suppress hepcidin, increasing iron absorption to facilitate red blood cell synthesis (Ganz, 2007). A recently identified hormone, erythroferrone, appears to play the most important role in stress erythropoiesis (Kautz *et al*, 2014). In thalassaemia intermedia syndromes, erythropoietic drive overwhelms negative feedback from iron overload, leading to iron absorption rates equal or exceeding many genetic haemochromatosis syndromes. In contrast, systemic inflammation promotes hepcidin release, lowering transferrin saturation (Walter *et al*, 2006). This physiological response acutely lowers iron bioavailability for invading pathogens but chronic inflammatory states create iron-restricted anaemia, independent of somatic iron stores (also known as anaemia of chronic disease) (Ganz, 2007).

While hepcidin regulates global iron homeostasis, organ iron levels are tightly regulated by molecular mechanisms at the cellular level (Fig 1, right). All cells need iron for maintenance of respiratory chain proteins and other important enzymes. Transferrin-bound iron is taken up by receptor-mediated endocytosis. When intracellular levels rise above optimal, iron regulatory proteins interact with iron response elements in genes for ferritin, transferrin receptor and ferroportin to upregulate safe iron storage, increase iron export- and limit further diferric transferrin uptake. Thus, it is essentially impossible for organs, such as the heart, endocrine glands and kidney, to become iron overloaded through transferrin- mediated iron uptake. As the liver is the dominant storage organ for excess iron, hepatocellular iron uptake of transferrin-bound iron is preserved even in iron overload conditions.

In severe iron overload, however, transferrin binding capacity becomes saturated and low molecular weight non-transferrin-bound iron (NTBI) or 'free' iron species appear

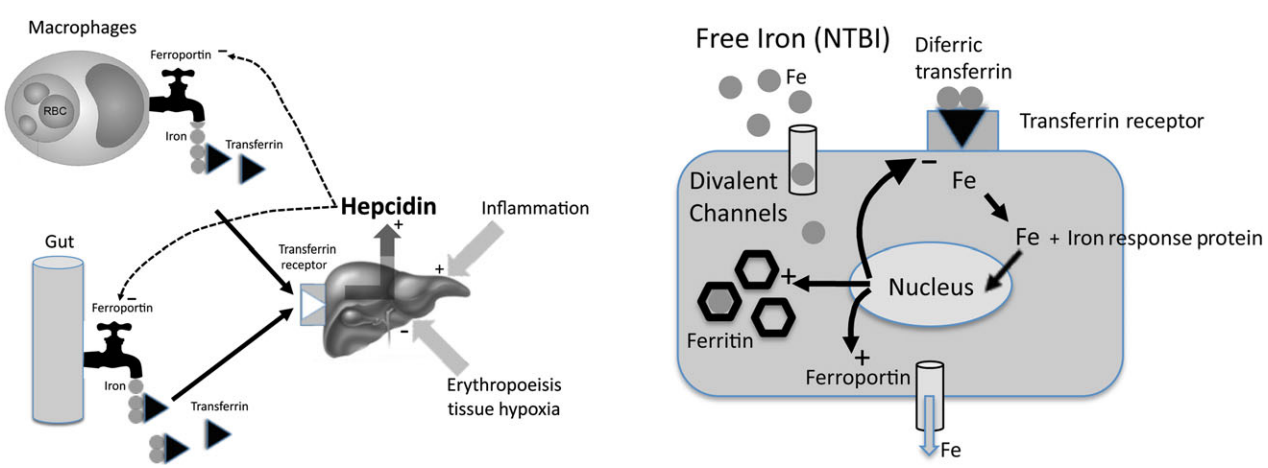

Fig 1. (Left) Schematic illustrating regulation of total body iron. Elevated iron flux through the gut and reticuloendothelial system increases transferrin saturation, upregulating hepcidin production in the liver. Hepcidin, by triggering internalization of ferroportin, limits iron export into the blood, serving as the central counter-regulatory mechanism. Erythropoietic drive suppresses hepcidin, thereby increasing iron flux from the gut and reticuloendothelial system. Inflammatory cytokines have the opposite effect. (Right) Schematic illustrating iron balance at the cellular level. When transferrin is not fully saturated, all iron entering parenchymal cells occurs through the transferrin receptor. Iron response proteins 'sense' intracellular iron, and modulate gene expression of transferrin receptor, ferritin, and ferroportin to properly balance import, storage and export of labile iron. When transferrin is fully saturated, circulating non-transferrin-bound iron (NTBI) can pass unrestricted through divalent cation channels, overwhelming the cells ability to store and export iron.

(Pootrakul *et al*, 2004; Piga *et al*, 2009). These positively charged moieties may circulate as complexes with citrate or loosely associated with proteins, such as albumin (Evans *et al*, 2008). Because of their small size, they are able to enter parenchymal cells readily through divalent metal channels (Oudit *et al*, 2006) and pinocytosis (Sohn *et al*, 2012). NTBI iron uptake is unregulated by iron response proteins, bypassing negative feedback mechanisms and increasing labile cellular iron pools (Cabantchik, 2014).

Although NTBI composes a very small fraction of body iron, it represents the toxic moiety that produces oxidative stress and organ damage. Total body iron stores are most closely reflected by liver iron (both hepatocyte and Kupffer cell) and spleen iron levels because they are the dominant iron storage organs (Morgan & Walters, 1963). In contrast, the heart and endocrine glands are sensitive to chronic exposure to NTBI species (Oudit *et al*, 2006). Transferrin saturation and NTBI levels, in turn, depend upon the disease state (Porter *et al*, 2014), transfusional rate (Inati *et al*, 2010), effective erythropoietic rate (Meloni *et al*, 2014; Porter *et al*, 2014) and ineffective erythropoietic rate (Kattamis *et al*, 2006), as well as the type and pattern of iron chelation (Zanninelli *et al*, 2009).

As a result, no simple relationships exist between total body iron burden and extrahepatic iron loading. Liver iron burdens exceeding 15–20 mg/g appear to place patients at increased cardiac risk (Brittenham *et al*, 1994; Wood *et al*, 2010, 2011a), but low liver iron levels do not guarantee cardiac protection (Noetzli *et al*, 2008). We reviewed results from routine cardiac and liver iron surveillance over 10 years and determined liver iron burden at the time that patients first developed detectable cardiac iron loading (Fig 2) (Wood, 2014). SCD patients only developed cardiac siderosis once they had severely loaded their livers. However, only 9/21 patients with thalassaemia major (TM) or rare anaemias (Other) with *de-novo* cardiac iron overload had liver iron concentration (LIC's) considered 'high risk' by previously published standards. These data demonstrate that control of total body iron burden is not sufficient for primary prevention of cardiac iron.

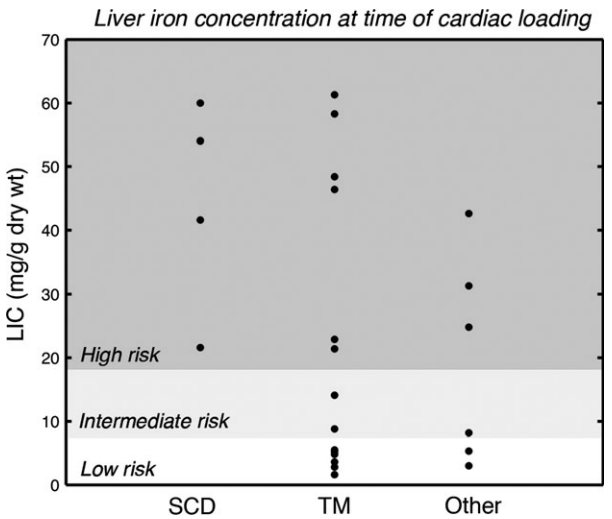

Fig 2. Distribution plot illustrating liver iron concentration (LIC) at the onset of primary cardiac iron loading in patients with sickle cell disease (SCD), thalassaemia major (TM) and other rare anaemias. Patients were undergoing routine clinical assessment of cardiac T2* and LIC at 1- to 2-year intervals. The onset of cardiac iron loading was defined as the time that a patient passed from a T2* > 20 ms to a T2* < 20 ms. Shaded areas depict 'classic' liver risk stratification, low (<7 mg/g), intermediate (7–15 mg/g) and high (>15 mg/g). In SCD patients, cardiac siderosis only developed in patients with extremely high LIC values. In contrast, a majority of TM and rare anaemia patients developed cardiac siderosis at LIC values considered 'low risk'. Figure reproduced from Wood (2014) with permission.

Monitoring iron overload

Measures of iron intake

Patients who are placed on chronic transfusion therapy accumulate iron at extremely predictable rates (Barry *et al*, 1974). As a rule of thumb, each transfusion of 15 ml/kg (assuming a haematocrit of 67%) will raise LIC by 1 mg/g dry weight (Cohen *et al*, 2008). Thus a patient placed on a 3-week transfusion cycle can expect LIC to increase 17 mg/g dry weight annually. In the absence of significant haemolysis (Inati *et al*, 2010), spontaneous iron losses are small, representing approximately one transfusion's worth of iron per year.

Characterizing transfusional rate is an effective way to estimate iron burden in the absence of chelation (Barry *et al*, 1974; Cohen *et al*, 2008; Inati *et al*, 2010; Ruccione *et al*, 2012) and useful in deciding when to initiate iron chelation therapy (Danjou *et al*, 2014). Unfortunately, intersubject variability in chelator efficacy and patient compliance limit the usefulness of transfusion rate once iron chelation has started (Cohen *et al*, 2008). Spontaneous iron losses can also be increased in patients with haemolytic disease (Inati *et al*, 2010).

Predicting intake in hyperabsorption disorders is more difficult than for transfusional haemochromatosis (Adams & Barton, 2007). Although hepcidin negative feedback is disrupted, it is not eliminated. Thus, iron absorption rates increase as iron stores are depleted through phlebotomy or chelation therapies.

Serum ferritin

Although imaging methods for quantifying iron are vital, the low cost and widespread availability of serum markers makes their use indispensible. Serum ferritin is the most widely used biomarker of iron status in the world. The biology of serum ferritin is poorly understood. Ferritin is primarily an intracellular protein produced to protect cells from labile intracellular iron (Brewer *et al*, 2014). Most of the circulating

ferritin fraction is released from the liver and does not contain iron. Chronically elevated serum ferritin levels are associated with poor outcomes in TM (Olivieri *et al*, 1994; Borgna-Pignatti *et al*, 2004). In patients with homozygous C282Y haemochromatosis, a serum ferritin level >1000 μg/l conveyed a fivefold risk of all-cause mortality, even with appropriate therapy (Barton *et al*, 2012).

Serum ferritin broadly tracks LIC, with an r^2 value of 50–64% in several studies (Brissot *et al*, 1981; Brittenham *et al*, 1993; Puliyel *et al*, 2014). While this statistical association is strong enough to predict mortality risk in thalassaemia cohorts, its predictive value for any individual is quite poor. Two patients with identical serum ferritin values can have vastly different iron burdens; for example, a patient with a serum ferritin of 2500 μg/l would have 95% confidence intervals for LIC between 5 and 25 mg/g, an enormous range with respect to risk of iron-mediated complications.

A number of biological processes modulate serum ferritin, including transfusion rate, systemic inflammation (Brittenham *et al*, 1993), ascorbate status (Chapman *et al*, 1982), liver disease (Kountouras *et al*, 2013) and rapid cell turnover. The relationship between ferritin and liver iron burden is particularly weak in nontransfused patients (Musallam *et al*, 2011). While a serum ferritin of 1000 μg/l is often considered acceptable in TM patients, the same level in a thalassaemia intermedia patient may be associated with life-threatening iron overload (Musallam *et al*, 2011). Recent work highlights guidelines for using serum ferritin in thalassaemia intermedia patients (Taher *et al*, 2015). In regions where LIC assessment is not feasible, they advocate iron chelation therapy for serum ferritin levels >800 μg/l, further dose escalation for ferritin >2000 μg/l and cessation of chelation when ferritin levels decrease below 300 μg/l.

Ascorbate deficiency lowers serum ferritin and transferrin saturation, presumably by limiting iron export from the reticuloendothelial system (Chapman *et al*, 1982; Brewer *et al*, 2012). Ascorbate deficiency is relatively common in iron overload syndromes (Chapman *et al*, 1982; Claster *et al*, 2009). Although partially protective of iron-mediated damage, the negative effects of vitamin C deficiency outweigh the benefits and careful ascorbate supplementation is warranted.

Ferritin is an acute phase reactant. Thus both systemic inflammation and acute liver injury raise serum ferritin out of proportion to somatic iron stores. In fact, the single most common cause of hyperferritinemia in the United States is metabolic syndrome (Kowdley *et al*, 2012). Although most haemoglobin disorders exhibit some degree of vascular inflammation from their iron overload, patients with SCD have the most striking systemic inflammation (Walter *et al*, 2006). Not surprisingly, correlations between serum ferritin and liver iron are significantly weaker in SCD, making ferritin even harder to interpret in these patients (Puliyel *et al*, 2014).

The accuracy of serum ferritin can be improved by measuring it frequently (every 3–6 weeks) and calculating a running average (Puliyel *et al*, 2014); this reduces the impact of transient increases produced by inflammation and acute hepatitis. Despite this approach, changes in serum ferritin and liver iron can by quite disparate over long periods of time. In a study of 134 patients followed by MRI for up to 9 years, trends in serum ferritin were discordant with LIC 26% of the time (Puliyel *et al*, 2014). As a result, anchoring of serum ferritin trends to gold-standard assessments of iron burden is highly recommended.

Serum markers of labile iron

Non-transferrin-bound iron burden is critically important to extrahepatic iron deposition and toxicity. The likelihood of detecting circulating NTBI increases dramatically once transferrin saturation exceeds 75–85% (Pootrakul *et al*, 2004; Piga *et al*, 2009). Transferrin saturation is a widely available clinical test and invaluable in the recognition and risk stratification of genetic haemochromatosis disorders (Adams & Barton, 2007). It is also a useful metric for deciding when to initiate iron chelation therapy in chronically transfused patients (Danjou *et al*, 2014). However, it has two key limitations. Firstly, it cannot be accurately assessed when iron chelators are present in the blood stream. Hence iron chelation must be withheld for two half-lives prior to blood sampling. Secondly, transferrin saturation codes patients as either high or low risk for cardiac siderosis, based on the 75–85% saturation cut-off, but does not provide graded risk stratification. While this information can be helpful in lower risk disease states, such as thalassaemia intermedia and SCD, it is less useful in TM where most patients will have transferrin saturation exceeding 85%.

Non-transferrin-bound iron can be directly measured using high-pressure liquid chromatography (Gosriwatana *et al*, 1999). Alternatively, the redox active fraction of NTBI, or labile plasma iron (LPI), can be measured using fluorescent labels (Breuer *et al*, 2000). Although intuitively appealing, these measurements suffer from three important limitations. Firstly, the assays are incompletely validated and suffer from poor inter-laboratory agreement (Jacobs *et al*, 2005). Secondly, there is little data linking elevated NTBI or LPI levels with adverse clinical outcomes (Piga *et al*, 2009; Zanninelli *et al*, 2009; Wood *et al*, 2011a). Lastly, all labile iron metrics reflect a short time horizon, making them vulnerable to dietary iron, acute inflammation and recent chelator use (Zanninelli *et al*, 2009). Thus, future clinical correlation is needed before these metrics can be recommended for routine monitoring purposes.

Liver iron as surrogate for total body iron

The liver and spleen represent the dominant iron storage organs in the body (Morgan & Walters, 1963). As a result, LIC represents the best single surrogate of changes in total body iron. Evidence of this relationship stems from studies

in unchelated, chronically transfused thalassaemia patients (Barry *et al*, 1974), chronically transfused and chronically chelated TM patients (Brittenham *et al*, 1994) and TM patients cured by bone marrow transplantation undergoing therapeutic phlebotomy (Angelucci *et al*, 2000). Although the relationship between total body iron and LIC has not been validated in other disease states, the physiological principles are disease-independent. As a result, annual LIC by liver biopsy became a popular means to monitor iron chelation therapy at some centres (Angelucci *et al*, 1995). In experienced hands, liver biopsy is safe, having a major bleeding rate of 0·5% (Angelucci *et al*, 1995). Nonetheless, it is unpopular with patients. Liver biopsy also suffers from significant sampling error, particularly in diseased livers (Villeneuve *et al*, 1996). Biopsy handling and processing can dramatically alter the results. For example, specimens that are paraffin embedded for histological confirmation, prior to biochemical analysis, produce systematically higher LIC estimates than freshly processed samples because the de-waxing process removes tissue lipids (Butensky *et al*, 2005). Consequently, liver biopsy results are difficult to compare across studies and across laboratories.

To improve patient acceptance of liver iron assessments a number of non-invasive approaches to liver iron quantification have been developed, including computerized tomography (CT) (Wood *et al*, 2011b), magnetic susceptometry (Brittenham *et al*, 1982; Nielsen *et al*, 2000; Gianesin *et al*, 2012), and MRI (Anderson *et al*, 2001; St Pierre *et al*, 2005; Wood *et al*, 2005a; Hankins *et al*, 2009; Garbowski *et al*, 2014).

Computerized tomography

Low-dose quantitative computed tomography (qCT) has a long history in evaluating bone density. Radiation exposure is typically less than 1 mSv, or approximately the exposure of one round-trip flight in North America. The attenuation of iron is higher than background tissue and accurate iron quantitation can be performed for LICs exceeding around 7 mg/g dry weight (Wood *et al*, 2011b). At lower iron concentrations, the intrinsic variability of liver attenuation masks changes introduced by iron. To correct for this, scanning can be performed at two different beam energies. While this concept has been validated in animals (Goldberg *et al*, 1982), and phantoms (Tsai *et al*, 2014), dual energy qCT for liver iron estimation has never been validated in humans. With the increased availability of dual-energy CT scanners for coronary calcium scoring, this approach warrants revisiting.

Susceptometers

Tissue iron is paramagnetic, which means that it strengthens any magnetic field to which it is exposed. By placing special receiving antennae near the patient, it is possible to measure the change in an applied magnetic field created by an iron-loaded liver. The receiving coils can either operate at extremely cold temperatures, known as superconducting quantum interference devices (SQUID) (Brittenham *et al*, 1982; Nielsen *et al*, 2000), or at room temperature (Gianesin *et al*, 2012). Both devices measure magnetic susceptibility which is then converted to an estimate of LIC using assumed values for tissue water concentration and the intrinsic magnetic susceptibility of haemosiderin (Fischer *et al*, 2006). In practice, these conversion factors are not well characterized, leading to some spectacular miscalculations of LIC by SQUID in one clinical trial (Fischer *et al*, 2006). With proper scaling, however, magnetic susceptometers produce accurate and reproducible estimates of LIC (Fischer *et al*, 2006). In general, measurement accuracy improves with iron levels; their greatest uncertainties occur in patients with near normal LIC. However, the biggest limitation of these devices is their availability, with only five instruments operational in the entire world. Susceptometers also only provide information regarding iron in the liver and spleen.

Magnetic resonance imaging

MRI has emerged as the dominant non-invasive modality for tissue iron quantification. First proof of principle was demonstrated in 1983 (Stark *et al*, 1983) but it wasn't until early in the 21st century that MRI imaging hardware and software were able to provide reproducible results over a large range of tissue iron (Anderson *et al*, 2001; St Pierre *et al*, 2005; Wood *et al*, 2005a). MRI images the magnetic effects of iron indirectly, through its influence on neighbouring water protons (Ghugre & Wood, 2011). When humans are placed in a MRI magnet, the induced magnetic field in the body is homogenous to a few parts per million. Tissue iron disrupts the magnetic field, causing these tissues to darken more readily during image formation, proportional to the iron present. This darkening process can be characterized by a half-life, called T2 or T2* depending on the type of imaging procedure (spin-echo or gradient-echo respectively). T2 and T2* are measured in units of milliseconds (ms). Alternatively, one can convert the time constants T2 and T2* to the rate constants R2 and R2* by forming a reciprocal:

$$R2 = 1000/T2$$

$$R2* = 1000/T2*,$$

where the factor of 1000 arises from a conversion between ms and seconds. The units of R2 and R2* are per second (/s) or Hz. R2 and R2* are directly proportional to tissue iron concentration, while T2 and T2* are inversely proportional.

In the early 2000s, patients were routinely attending for liver biopsy as part of clinical care, making it relatively straightforward to validate R2- and R2*-based LIC estimates (St Pierre *et al*, 2005; Wood *et al*, 2005a). Figure 3 (left) summarizes the relationship between liver R2* and biopsy

from the three largest validation studies; biopsy data from an earlier study (Anderson *et al*, 2001) have largely been discredited because of inadequate acquisition methodology and biopsy standardization. The Wood and Hankins data are superimposable (Wood *et al*, 2005a Hankins *et al*, 2009). Small systematic differences between those studies and the data reported by Garbowski *et al* (2014) are observed for LIC's exceeding 20 mg/g, arising from differences in R2* curve fitting (Meloni *et al*, 2013). However, both processing approaches yield identical LIC estimates when appropriate calibration curves are used (Meloni *et al*, 2013). Figure 3 (right) summarizes the original data validating R2 (St Pierre *et al*, 2005), and confirmatory data from our group later that year (Wood *et al*, 2005a); agreement between the two studies is excellent. R2 has a more marked downward curvature to the R2-LIC relationship (St Pierre *et al*, 2005).

Neither R2 nor R2* perfectly represent LIC. While much of the scatter in the R2*-LIC and R2-LIC representations (Fig 3) arises from intrinsic sampling variability from liver biopsy, both R2 and R2* are indirect measures of tissue iron, introducing patient-specific uncertainties in LIC concentration. As a result, individual estimates of LIC by R2 and by R2* do not agree perfectly with one another, and should not be interchanged (Garbowski *et al*, 2014; Wood *et al*, 2014). However, both R2 and R2* have excellent inter-study reproducibility, of the order of 5–7% (St Pierre *et al*, 2005; Wood *et al*, 2005a). Inter-reader variability is low and results are highly reproducible across machine platforms (Westwood *et al*, 2003; Tanner *et al*, 2006). For this reason, serial measurements of R2 and R2* are better indicators of chelator effectiveness than can be obtained by liver biopsy (Wood *et al*, 2013). Trends in LIC predicted by both modalities agree closely with one another and either approach is suitable for clinical management (Wood *et al*, 2013, 2014). A third imaging technique, known as signal intensity ratios, can also be used for screening in patients with milder iron overload and is discussed in greater detail later in this review.

*Measurement of cardiac T2**

The heart and endocrine glands make up only a tiny fraction of the total body iron burden but produce the lion's share of complications (Borgna-Pignatti *et al*, 2004). Furthermore, as these organs exclusively accumulate NTBI, it is possible for them to be in positive iron balance even if the total body iron balance is neutral or negative (Noetzli *et al*, 2008). For example, LIC can easily be maintained at safe level by administering continuous high dose deferoxamine (DFO) for 2 d every 1–2 weeks (Wali *et al*, 2004); this strategy was briefly popular at our institution for very noncompliant patients. Unfortunately, NTBI levels in the blood rebound quickly after DFO infusions are halted (Porter *et al*, 1996), leaving the heart and endocrine glands unprotected. While this represents a management extreme, variations in chelator type, dosing and compliance, can have profound effects on the NTBI exposure to extrahepatic organs (Zanninelli *et al*, 2009).

The ability of MRI to detect and quantify tissue iron burden in the heart and endocrine glands has dramatically altered our ability to prevent iron toxicity in extrahepatic organs (Wood, 2009). Prior to their introduction in 2001, iron cardiomyopathy was the leading cause of death in TM (Borgna-Pignatti *et al*, 2004), with a mean age of survival of only 35 years in a large UK registry (Modell *et al*, 2000). Even with meticulous screening with radionuclide techniques and aggressive rescue strategies with continuous DFO, 35%

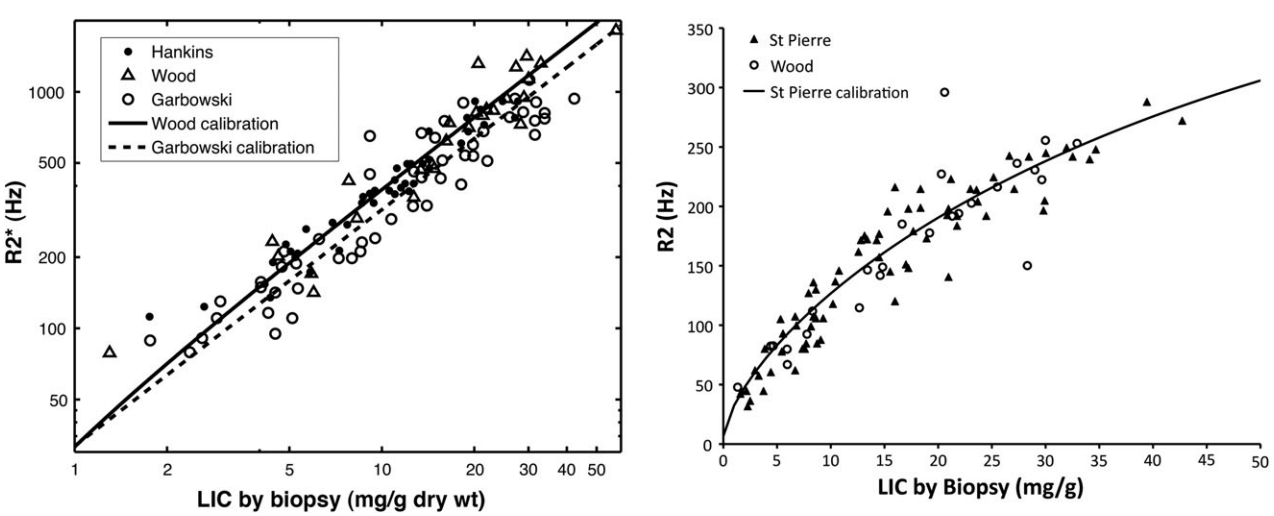

Fig 3. (Left) Plot of liver R2* *versus* liver iron concentration (LIC) by biopsy from three validation studies. Both axes are on a logarithmic scale. Data derived from primary sources (Wood *et al*, 2005a; Hankins *et al*, 2009; Garbowski *et al*, 2014). Calibration curves reproduced from published equations (Wood *et al*, 2005a; Garbowski *et al*, 2014). (Right) Plot of liver R2 *versus* LIC by biopsy from two validation studies. Axes are linear. Data derived from primary sources (St Pierre *et al*, 2005; Wood *et al*, 2005a). Calibration curve reproduced from published equation (St Pierre *et al*, 2005).

of patients who presented with asymptomatic cardiac dysfunction died (Davis & Porter, 2000). There were two key problems: (i) cardiac symptoms develop very late in the disease cascade and (ii) cardiac iron can take three or 4 years to clear from a heavily loaded heart, requiring unwavering compliance with intensive chelation strategies (Davis & Porter, 2000; Anderson *et al*, 2004).

In a landmark study, Anderson *et al* (2001) demonstrated that thalassaemia patients having normal cardiac T2* universally exhibited normal, or supranormal (Westwood *et al*, 2007) left ventricular function (Anderson *et al*, 2001). As the heart developed progressive iron loading (T2* < 20 ms), the prevalence of cardiac dysfunction increased.

Many patients in that study demonstrated MRI-detectable iron but normal function. The reason for this is that MRI primarily measures the safely stored haemosiderin iron (Wood *et al*, 2005b). However, a subsequent registry study demonstrated that that the prospective risk of developing congestive heart failure in thalassaemia patients was strongly dependent on cardiac T2* (Kirk *et al*, 2009), suggesting that stored iron predisposes patients to toxic labile intracellular iron. In fact, more than 50% of patients having cardiac T2* less than 6 ms developed overt heart failure in 1 year. Cardiac failure was exceeding rare in patients having cardiac T2* greater than 10 ms.

Cardiac T2* assessment has been transformative. With the ability to recognize preclinical cardiac iron accumulation, clinicians were able to implement primary prevention strategies for cardiac failure. In addition, cardiac T2* became an important biomarker to evaluate different iron chelation regimens (Pennell *et al*, 2006, 2010; Wood *et al*, 2010). In particular, chelator combinations became increasing popular, leading to improved patient outcomes (Tanner *et al*, 2007, 2008).

Unlike liver MRI measurements, cardiac T2* was validated clinically (Anderson *et al*, 2001; Kirk *et al*, 2009) before it was validated biochemically (Wood *et al*, 2005c; Ghugre *et al*, 2006; Carpenter *et al*, 2011). Initial validation was performed in gerbils (Wood *et al*, 2005c) and later validated in autopsy studies (Ghugre *et al*, 2006; Carpenter *et al*, 2011). Even with a known calibration curve, many studies continue to report results in T2* units, rather than iron levels, because the clinical community is more familiar with the results.

Other approaches to measuring cardiac iron

Although cardiac T2* represents the clinical standard of care, cardiac T2, T1 and so-called 'reduced-R2' measurements are being explored as potential biomarkers (He *et al*, 2009; Feng *et al*, 2013). T2 is tightly correlated with cardiac T2*, r^2 of 0·89 (He *et al*, 2009; Feng *et al*, 2013) for T2* < 20 ms, but the relationship becomes nonlinear at higher T2* values. T2 is less sensitive to long range susceptibility artefacts (He *et al*, 2009), allowing more of the heart to be used in forming the iron estimate.

Cardiac T1 measurements also are proportional to cardiac T2*, with r-values of 0·79–0·83 (Feng *et al*, 2013; Sado *et al*, 2014). T1 measurements also allow use of the entire left ventricular wall and may have better reproducibility than cardiac T2* measurements. However, neither T1 nor T2 measurements are universally available, they are less sensitive to changes in cardiac iron and they are not standardized across imaging platforms, so further work is needed to characterize their utility.

Reduced-R2 measurements represent an interesting approach to try to distinguish contributions from large iron aggregates (haemosiderin) from soluble ferritin. The theory and *in-vitro* data supporting this approach are complicated and the reader is referred to a key reference on this technique (Jensen & Chandra, 2002). Proof of concept has been demonstrated in iron overloaded patients exposed to 1 week interruption of iron chelation therapy (Kim *et al*, 2011). However, the image acquisition techniques for this approach are highly customized, limiting the generalizability of this approach.

*Measurements of pancreas R2**

While cardiac T2* is an early 'biomarker' for the risk of cardiac dysfunction, it is a relatively late indicator of endocrine risk. Figure 4 demonstrates the prevalence of hypogonadatrophic hypogonadism and glucose dysregulation as a function of cardiac and pancreatic iron deposition. The heart and pancreas both exclusively accumulate NTBI (Oudit *et al*, 2006), but the pancreas appears to do so earlier, serving as a 'early warning system' for inadequate suppression of circulating NTBI (Noetzli *et al*, 2009; Pfeifer *et al*, 2014). The relationship is sufficiently strong and independent of disease state (Meloni *et al*, 2014), that our laboratory no longer performs cardiac T2* assessment in patients who have a pancreas R2* less than 100 Hz.

Normal pancreas R2* is <40 Hz (Restaino *et al*, 2011). Patients with pancreas R2* > 100 Hz, but normal cardiac iron, also have increased risk of glucose dysregulation (Noetzli *et al*, 2012b). The relationship between pancreas R2* and diabetes is complicated by the multiple effects of iron on glucose regulation and the interplay between insulin sensitivity and release (Bergman *et al*, 2002; Noetzli *et al*, 2012b). Pancreas R2* is clearly the strongest predictor of beta cell function, but age, body mass index and LIC of the patient also contribute (Noetzli *et al*, 2012b). Given that endocrine damage may take decades to manifest itself and that abnormal oral glucose tolerance tests do not occur until there is significant beta cell damage (Bergman *et al*, 2002), it makes intuitive sense to use pancreas R2* values to guide primary prevention. However, longitudinal data relating pancreas R2* to diabetes risk are lacking and it will require many patient-years of observation to confirm this hypothesis.

Measurement of pancreas R2* does not take additional imaging time in patients undergoing liver R2* analysis

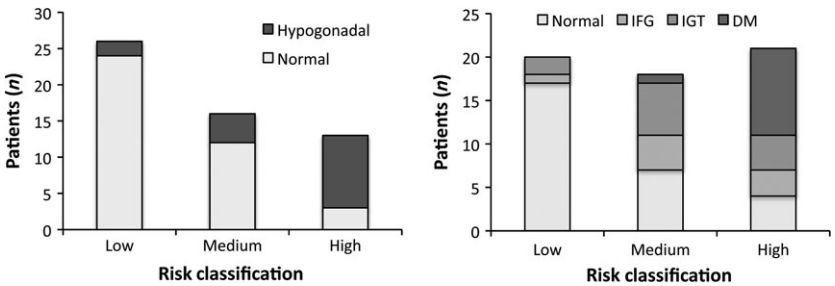

Fig 4. Prevalence of clinical hypogonadism (left) and abnormal glucose tolerance (right) as a function of pancreas and cardiac iron metrics. Low risk patients are defined as having no detectable cardiac iron (T2* > 20 ms) and a pancreas R2* < 100 Hz. Intermediate risk patients have increased pancreas iron (R2* > 100 Hz) but no cardiac siderosis. High risk patients have cardiac siderosis (all of them also have pancreas R2* > 100 Hz). Both hypogonadism and diabetes are extremely common in patients with cardiac siderosis, indicating that cardiac iron is a late manifestation of poor non-transferrin-bound iron control. Pancreatic iron deposition, in the absence of cardiac iron overload, also conveys an intermediate risk of both pituitary and pancreatic dysfunction. Figures derived from data presented previously (Noetzli *et al*, 2012a,b). IFG, impaired fasting glucose; IGT, impaired glucose tolerance; DM, diabetes mellitus.

(Restaino *et al*, 2011); the pancreas can often be visualized in axial slices between the costophrenic angle and the porta hepatits. Quantification is easy in children and young adults but can be more difficult in middle age because of fatty infiltration of the pancreas. The use of fat saturation techniques can make pancreas R2* estimation more robust.

Measurement of pituitary iron

The pituitary gland can accumulate dangerous levels of iron in the first decade of life (Noetzli *et al*, 2012a). Unfortunately, pituitary gonadotropic function cannot be assessed until puberty, when potentially irreversible damage may have already occurred. Both pituitary R2 values and pituitary size are validated biomarkers of pituitary function (Argyropoulou *et al*, 2000, 2001; Noetzli *et al*, 2012a). R2 and volume values vary with age and sex, but simple nomograms are available to convert them into Z-scores (normal is $-2 \leq Z \leq 2$) (Noetzli *et al*, 2012c). In a cross sectional study of 56 chronically transfused thalassaemia or Blackfan Diamond patients, loss of pituitary volume (Z score less than -2) was highly specific for hypogonadatrophic hypogonadism (Noetzli *et al*, 2012a). Moderate pituitary iron loading (Z score < 5), with normal gland volume, was not associated with clinical hypogonadism but more than 50% of patients having pituitary iron burdens greater than this threshold were hypogonadal (Noetzli *et al*, 2012a). Further studies will be necessary to determine whether pituitary function could be 'rescued' in these patients using intensive chelation therapy, as has been proposed by Farmaki *et al* (2010).

Measurement of pituitary R2 is straightforward and does not require specialized software for analysis. Measurement of pituitary volume requires manual planimetry but is not difficult (Noetzli *et al*, 2012c). Some advocate the use of pituitary height as surrogate for volume for speed and simplicity (Argyropoulou *et al*, 2001), but we do not support this because the pituitary gland can be irregularly shaped. Total imaging time is under 8 min.

To date, pituitary imaging has been limited to research studies. While it would appear to be a logical approach to guide primary prevention of hypogonadism, larger clinical experience with these techniques is necessary prior to considering them as standard of care.

Protocols for monitoring

No evidence-based evaluations of monitoring protocols exist although a number of consensus based protocols have been published. The following represent that clinical practices at Children's Hospital Los Angeles; consensus protocols have been referenced when appropriate. Our patient population reflects approximately 50% chronically transfused SCD, 25% TM and 25% other chronic anaemias including Blackfan Diamond Syndrome, congenital dyserythropoietic anaemia, aplastic anaemia, pure red cell aplasia, PK deficiency, thalassaemia intermedia and anaemia secondary to chemotherapy. Only three patients have myelodysplasia and guidelines for these patients should integrate co-morbidities, life-expectancy and quality of life issues.

All patients undergoing regular transfusion therapy have frequent monitoring (every or every other transfusion) of serum ferritin, together with abdominal MRI examinations every 1–2 years (Puliyel *et al*, 2014). In non-transfused iron overload syndromes, MRI is performed at baseline and sporadically (every 5 years) during maintenance iron removal therapy to confirm therapy adequacy.

Figure 5 represents a schematic illustrating our general clinical practice. Patients at low risk for cardiac iron overload and without significant pancreatic iron deposition can continue to be monitored with abdominal MRI alone. All patients with pancreas R2* greater than 100 Hz are considered 'standard' risk and have liver and cardiac iron assessments on a 12- to 24-month basis (Pennell *et al*, 2013).

Patients with documented cardiac T2* less than 10 ms are considered 'high risk' and undergo heart and liver assessments every 6 months to guide intensified iron chelation

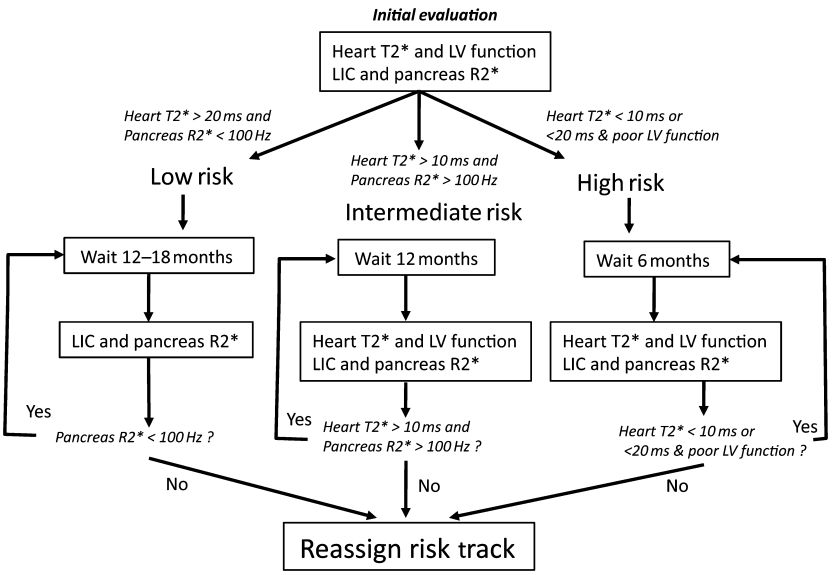

Fig 5. Algorithm depicting our routine iron surveillance practices. Based upon our initial complete iron assessment, patients are assigned to one of three tracks based upon the perceived risk of developing cardiac iron. Risk stratification is the same as shown in Fig 4. Graph redrawn from prior work (Wood, 2014). LIC, liver iron concentration; LV, left ventricular. Figure adapted from Wood (2014) with permission.

therapy (Pennell *et al*, 2013). We also consider patients with ventricular dysfunction and cardiac T2* between 10 and 20 ms to also be 'high risk'.

Apriori *stratification of cardiac risk*

Classification of 'high' and 'low' cardiac risk based upon underlying disease states and physiology is an evolving topic. Guiding principles and broad stratification of iron overload states are summarized in Fig 6 (left). In general, factors that increase NTBI exposure increase cardiac risk. These include increased transfusion rate (increased iron flux), ineffective erythropoiesis (hepcidin suppression) (Kattamis *et al*, 2006), liver damage [decreased NTBI reabsorption (Cabantchik, 2014) and hepcidin suppression] and possibly splenectomy (loss of iron storage capacity). In contrast, effective erythropoiesis is protective, by regenerating apotransferrin and lowering transferrin saturation; this is probably the strongest single determinate of cardiac risk (Meloni *et al*, 2014; Porter *et al*, 2014). Chronic inflammation (increased hepcidin) (Walter *et al*, 2006) and ascorbate deficiency (decreased release from reticuloendothlial macrophages) also lower cardiac risk (Brewer *et al*, 2012).

Based on these considerations, non-transfused iron overload syndromes are at the lowest risk, rarely developing cardiac iron before the age 30–40 years (Roghi *et al*, 2010)

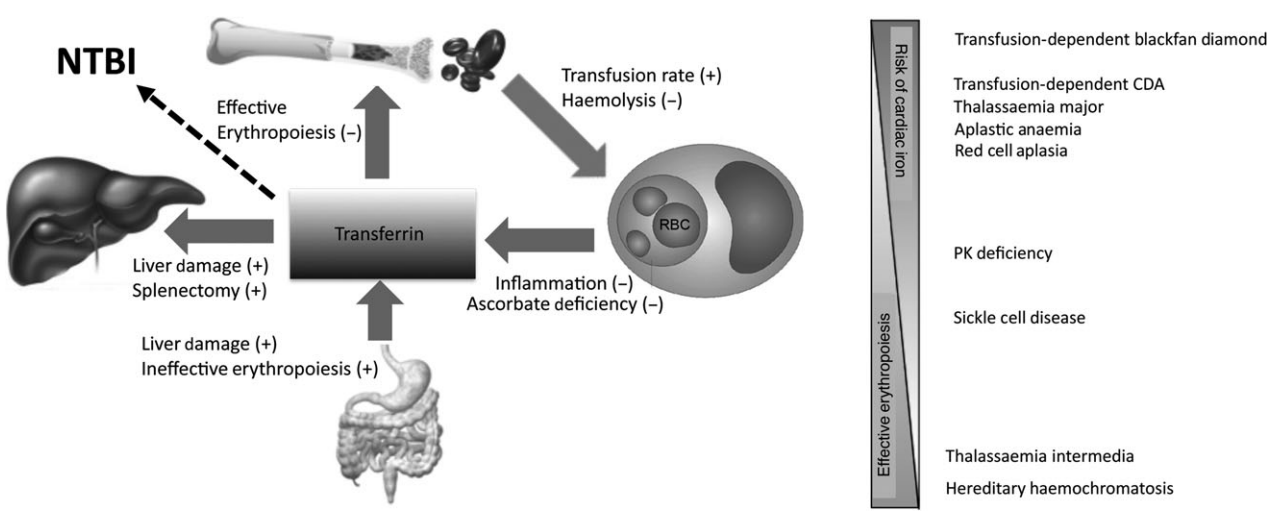

Fig 6. (Left) Schematic depiction of the global iron homeostasis, illustrating factors that modulate transferrin saturation and the risk of non-transferrin-bound iron (NTBI) and extrahepatic iron deposition. Plus and minus signs depict the impact of a particular process on NTBI, not on hepcidin secretion. For example, effective erythropoiesis *increases* bone marrow uptake of transferrin, regenerating apotransferrin and thereby *lowering* NTBI. (Right) Approximate ranking of cardiac risk across disease states; CDA is an abbreviation for congenital dyserythropoetic anemia. In general, cardiac risk is reciprocally related to absolute effective erythropoetic rate.

(Fig 6, right). Juvenile haemochromatosis represents an exception to this rule; their iron absorption rates are so torrential that transferrin saturates in early childhood despite effective erythropoiesis, leading to pancreatic and cardiac iron in early adolescence. Chronically transfused patients with SCD are also at low risk, despite significant total body iron burdens, because effective reticulocyte generation lowers transferrin saturation (Meloni *et al*, 2014). In contrast, transfusion-dependent Blackfan Diamond syndrome and congenital dyserythropoetic anaemias (CDAs) represent the other end of the spectrum (Porter, 2007; Wood, 2008). The near absence of marrow iron utilization in these diseases causes high circulating NTBI levels and early extrahepatic iron deposition (Porter, 2007; Wood, 2008; Berdoukas *et al*, 2013; Porter *et al*, 2014). However, patients with Blackfan Diamond and CDA are not always transfusion-dependent, and such patients have lower cardiac risk. Some anemias, such as myelodysplastic syndrome, may decrease effective erythropoiesis over time, potentially increasing cardiac risk because of increased iron input (transfusions) and decreased utilization of transferrin-bound iron. Other rare anaemias have such heterogeneous phenotypes and interacting physiological influences on NTBI exposure that cardiac risk is difficult to assess *apriori*.

Another important key modifier of cardiac risk is the duration of exposure to circulating NTBI. Cardiac iron accumulation is markedly delayed compared with other organs, including the liver and pancreas (Noetzli *et al*, 2009). However, cardiac iron overload can progress quite rapidly once it starts (Noetzli *et al*, 2008). The mechanisms responsible for organ-specific loading dynamics remain unclear.

Practical considerations for monitoring

There are three general approaches to measuring LIC by MRI, signal intensity ratios (SIR), Ferriscan-R2 and R2* assessments; the advantages and disadvantages of these approaches are summarized in Table I.

Signal intensity ratios represent the simplest approach. Characteristic gradient echo image series of the abdomen are collected in five breath-holds. Regions of interest are drawn in the liver and paraspinous muscles. Values are entered into a free website (http://www.radio.univrennes1.fr/Sources/EN/HemoCalc15.html) to generate LIC estimates. Calibrations were derived from a large cohort of liver biopsies from patients with primary hyperabsorption disorders (Gandon *et al*, 1994). The primary advantages of this approach are its ease and inexpensiveness. The web-based calculations have not been approved by the US Food and Drug Administration, which may present a regulatory issue for some Radiology departments. However, the more important limitation of SIR's is that they are really only robust for low iron concentrations. Although modifications have been introduced to try to broaden the dynamic range (Rose *et al*, 2006), the fundamental assumptions of the signal intensity approach are violated at high iron concentration and relaxometry (R2 or R2*) becomes the modality of choice. Nonetheless, SIR approaches represent a viable option for screening purposes in primary haemochromatosis syndromes, particularly if relaxometry is not feasible; many sites use this approach worldwide.

Table I. Comparison of MRI methods to evaluate LIC.

LIC by Ferriscan R2	LIC by R2*	LIC by SIR
Advantages	*Advantages*	*Advantages*
Good quality control	Fast	Widely available
Well validated	Temporally stable	Free
Disadvantages	*Disadvantages*	*Disadvantages*
Expensive	Need local expertise	Poor dynamic range
Sensitive to iron distribution	Need validated software	Greater variability
Longer examination time	Smaller dynamic range	
Examinations may need repeating		

MRI, magnetic resonance imaging; LIC, liver iron concentration; SIR, signal intensity ratios.

Ferriscan-R2 is an outsourced, standardized spin-echo and analysis pipeline designed by Dr. Tim St Pierre (St Pierre *et al*, 2005, 2014) and maintained by a private company (Resonance Health, Western Australia, http://www.resonance-health.com/). Quality control includes technician training manuals, scanning of a test object, strict checks of sequence parameters and inspection of image quality. Primary advantages of Ferriscan are its convenience and quality control, but it comes at a price of approximately €250–300.

Liver R2* is a faster and more versatile relaxometry technique as other abdominal organs can be analysed at the same time. R2* is fundamentally more robust to fluctuations in iron distribution within the liver and has better temporal stability when examinations are performed at intervals shorter than 1 year (Wood *et al*, 2013, 2014). However, quality control must be enforced locally, requiring radiological and/or engineering support. Validated software is needed to measure R2* from the images. Lastly, liver R2* is only capable of imaging LIC levels up to 35 or 40 mg/g, depending on the MRI scanner.

R2 and R2* have superb inter-study and cross-platform reproducibility, making then fundamentally more accurate than liver biopsy for assessment of iron chelation efficacy (Wood *et al*, 2013, 2014). Thus choice of liver iron measurement techniques is driven primarily by the motivation of individual radiology services to support the measurements and the patient population requiring imaging surveillance.

Cardiac T2* measurements are collected using the same acquisition software as for liver R2* measurements. Images can be collected with or without a special radiofrequency pulse that turns the blood black on the MRI image (black

blood T2* image). While a black-blood cardiac T2* sequence has slightly better inter-study reproducibility, white blood imaging produces clinically acceptable quantitation. Image analysis can be outsourced to Resonance Health for a fee, or analysed locally using the same software as for liver R2* analysis.

Iron quantification should be performed on 1·5 Tesla magnets whenever possible because the measurements are better validated and more robust. R2 and R2* values increase with magnetic field strength (Storey *et al*, 2007) and calibration curves must be adjusted for these effects. Three Tesla (3T) magnets have advantages when tissue iron levels are low and imaging resolution is imperative, such as for brain or pituitary iron quantitation. However, artefacts are worse at 3T, particularly in the abdomen, and severe hepatic iron loading (greater than 15 or 20 mg/g) cannot be measured.

Acknowledgements

This work supported by the National Institutes of Health, National Institute of Diabetes and Digestive and Kidney Diseases (1R01DK097115-01A1) and the National Heart Lung and Blood Institute (1U01HL117718-01). Dr Wood has served as a MRI consultant to Shire and is a MRI consultant to BiomedInformatics. The author is grateful for the contributions of the clinical haematology program at Children's Hospital Los Angeles, his co-investigators, and his research staff.

References

Adams, P.C. & Barton, J.C. (2007) Haemochromatosis. *Lancet*, **370**, 1855–1860.

Anderson, L.J., Holden, S., Davis, B., Prescott, E., Charrier, C.C., Bunce, N.H., Firmin, D.N., Wonke, B., Porter, J., Walker, J.M. & Pennell, D.J. (2001) Cardiovascular T2-star (T2*) magnetic resonance for the early diagnosis of myocardial iron overload. *European Heart Journal*, **22**, 2171–2179.

Anderson, L.J., Westwood, M.A., Holden, S., Davis, B., Prescott, E., Wonke, B., Porter, J.B., Malcolm Walker, J. & Pennell, D.J. (2004) Myocardial iron clearance during reversal of siderotic cardiomyopathy with intravenous desferrioxamine: a prospective study using T2* cardiovascular magnetic resonance. *British Journal of Haematology*, **127**, 348–355.

Angelucci, E., Baronciani, D., Lucarelli, G., Baldassarri, M., Galimberti, M., Giardini, C., Martinelli, F., Polchi, P., Polizzi, V. & Ripalti, M. (1995) Needle liver biopsy in thalassaemia: analyses of diagnostic accuracy and safety in 1184 consecutive biopsies. *British Journal of Haematology*, **89**, 757–761.

Angelucci, E., Brittenham, G.M., McLaren, C.E., Ripalti, M., Baronciani, D., Giardini, C., Galimberti, M., Polchi, P. & Lucarelli, G. (2000) Hepatic iron concentration and total body iron stores in thalassemia major. *New England Journal of Medicine*, **343**, 327–331.

Argyropoulou, M.I., Metafratzi, Z., Kiortsis, D.N., Bitsis, S., Tsatsoulis, A. & Efremidis, S. (2000) T2 relaxation rate as an index of pituitary iron overload in patients with beta-thalassemia major. *American Journal of Roentgenology*, **175**, 1567–1569.

Argyropoulou, M.I., Kiortsis, D.N., Metafratzi, Z., Bitsis, S., Tsatoulis, A. & Efremidis, S.C. (2001) Pituitary gland height evaluated by MR in patients with beta-thalassemia major: a marker of pituitary gland function. *Neuroradiology*, **43**, 1056–1058.

Barry, M., Flynn, D., Letsky, E.A. & Risdon, R.A. (1974) Long-term chelation therapy in thalassemia major: effect on LIC, liver histology, and clinical progress. *British Medical Journal*, **2**, 16–20.

Barton, J.C., Barton, J.C., Acton, R.T., So, J., Chan, S. & Adams, P.C. (2012) Increased risk of death from iron overload among 422 treated probands with HFE hemochromatosis and serum levels of ferritin greater than 1000 μg/L at diagnosis. *Clinical Gastroenterology and Hepatology*, **10**, 412–416.

Berdoukas, V., Nord, A., Carson, S., Puliyel, M., Hofstra, T., Wood, J. & Coates, T.D. (2013) Tissue iron evaluation in chronically transfused children shows significant levels of iron loading at a very young age. *American Journal of Hematology*, **88**, E283–E285.

Bergman, R.N., Finegood, D.T. & Kahn, S.E. (2002) The evolution of beta-cell dysfunction and insulin resistance in type 2 diabetes. *European Journal of Clinical Investigation*, **32**, 35–45.

Borgna-Pignatti, C., Rugolotto, S., De Stefano, P., Zhao, H., Cappellini, M.D., Del Vecchio, G.C., Romeo, M.A., Forni, G.L., Gamberini, M.R., Ghilardi, R., Piga, A. & Cnaan, A. (2004) Survival and complications in patients with thalassemia major treated with transfusion and deferoxamine. *Haematologica*, **89**, 1187–1193.

Breuer, W., Ronson, A., Slotki, I.N., Abramov, A., Hershko, C. & Cabantchik, Z.I. (2000) The assessment of serum nontransferrin-bound iron in chelation therapy and iron supplementation. *Blood*, **95**, 2975–2982.

Brewer, C., Otto-Duessel, M., Lykkesfeldt, J., Nick, H. & Wood, J.C. (2012) Ascorbate status modulates reticuloendothelial iron stores and response to deferasirox iron chelation in ascorbate-deficient rats. *Experimental Hematology*, **40**, 820–827.

Brewer, C.J., Wood, R.I. & Wood, J.C. (2014) mRNA regulation of cardiac iron transporters and ferritin subunits in a mouse model of iron overload. *Experimental Hematology*, **42**, 1059–67.

Brissot, P., Bourel, M., Herry, D., Verger, J.P., Messner, M., Beaumont, C., Regnouard, F., Ferrand, B. & Simon, M. (1981) Assessment of liver iron content in 271 patients: a reevaluation of direct and indirect methods. *Gastroenterology*, **80**, 557–565.

Brittenham, G.M., Farrell, D.E., Harris, J.W., Feldman, E.S., Danish, E.H., Muir, W.A., Tripp, J.H. & Bellon, E.M. (1982) Magnetic-susceptibility measurement of human iron stores. *New England Journal of Medicine*, **307**, 1671–1675.

Brittenham, G.M., Cohen, A.R., McLaren, C.E., Martin, M.B., Griffith, P.M., Nienhuis, A.W., Young, N.S., Allen, C.J., Farrell, D.E. & Harris, J.W. (1993) Hepatic iron stores and plasma ferritin concentration in patients with sickle cell anemia and thalassemia major. *American Journal of Hematology*, **42**, 81–85.

Brittenham, G.M., Griffith, P.M., Nienhuis, A.W., McLaren, C.E., Young, N.S., Tucker, E.E., Allen, C.J., Farrell, D.E. & Harris, J.W. (1994) Efficacy of deferoxamine in preventing complications of iron overload in patients with thalassemia major. *New England Journal of Medicine*, **331**, 567–573.

Butensky, E., Fischer, R., Hudes, M., Schumacher, L., Williams, R., Moyer, T.P., Vichinsky, E. & Harmatz, P. (2005) Variability in hepatic iron concentration in percutaneous needle biopsy specimens from patients with transfusional hemosiderosis. *American Journal of Clinical Pathology*, **123**, 146–152.

Cabantchik, Z.I. (2014) Labile iron in cells and body fluids: physiology, pathology, and pharmacology. *Fronteirs in Pharmacology*, **5**, 45.

Carpenter, J.P., He, T., Kirk, P., Roughton, M., Anderson, L.J., de Noronha, S.V., Sheppard, M.N., Porter, J.B., Walker, J.M., Wood, J.C., Galanello, R., Forni, G., Catani, G., Matta, G., Fucharoen, S., Fleming, A., House, M.J., Black, G., Firmin, D.N., St Pierre, T.G. & Pennell, D.J. (2011) On T2* magnetic resonance and cardiac iron. *Circulation*, **123**, 1519–1528.

Chapman, R.W., Hussain, M.A., Gorman, A., Laulicht, M., Politis, D., Flynn, D.M., Sherlock, S. & Hoffbrand, A.V. (1982) Effect of ascorbic acid deficiency on serum ferritin concentration in patients with beta-thalassaemia major and iron overload. *Journal of Clinical Pathology*, **35**, 487–491.

Claster, S., Wood, J.C., Noetzli, L., Carson, S.M., Hofstra, T.C., Khanna, R. & Coates, T.D. (2009) Nutritional deficiencies in iron overloaded patients with hemoglobinopathies. *American Journal of Hematology*, **84**, 344–348.

Cohen, A.R., Glimm, E. & Porter, J.B. (2008) Effect of transfusional iron intake on response to chelation therapy in beta-thalassemia major. *Blood*, **111**, 583–587.

Corradini, E., Meynard, D., Wu, Q., Chen, S., Ventura, P., Pietrangelo, A. & Babitt, J.L. (2011) Serum and liver iron differently regulate the bone morphogenetic protein 6 (BMP6)-SMAD signaling pathway in mice. *Hepatology*, **54**, 273–284.

Danjou, F., Cabantchik, Z.I., Origa, R., Moi, P., Marcias, M., Barella, S., Defraia, E., Dessi, C., Foschini, M.L., Giagu, N., Leoni, G.B., Morittu, M. & Galanello, R. (2014) A decisional algorithm to start iron chelation in patients with beta thalassemia. *Haematologica*, **99**, e38–e40.

Davis, B.A. & Porter, J.B. (2000) Long-term outcome of continuous 24-hour deferoxamine infusion via indwelling intravenous catheters in high-risk beta-thalassemia. *Blood*, **95**, 1229–1236.

Evans, R.W., Rafique, R., Zarea, A., Rapisarda, C., Cammack, R., Evans, P.J., Porter, J.B. & Hider, R.C. (2008) Nature of non-transferrin-bound iron: studies on iron citrate complexes and thalassemic sera. *Journal of Biological Inorganic Chemistry*, **13**, 57–74.

Farmaki, K., Tzoumari, I., Pappa, C., Chouliaras, G. & Berdoukas, V. (2010) Normalisation of total body iron load with very intensive combined chelation reverses cardiac and endocrine complications of thalassaemia major. *British Journal of Hematology*, **148**, 466–475.

Feng, Y., He, T., Carpenter, J.P., Jabbour, A., Alam, M.H., Gatehouse, P.D., Greiser, A., Messroghli, D., Firmin, D.N. & Pennell, D.J. (2013) In vivo comparison of myocardial T1 with T2 and T2* in thalassaemia major. *Journal of Magnetic Resonance Imaging*, **38**, 588–593.

Fischer, R., Harmatz, P. & Nielsen, P. (2006) Does liver biopsy overestimate liver iron concentration? *Blood*, **108**, 778.

Gandon, Y., Guyader, D., Heautot, J.F., Reda, M.I., Yaouanq, J., Buhe, T., Brissot, P., Carsin, M. & Deugnier, Y. (1994) Hemochromatosis: diagnosis and quantification of liver iron with gradient-echo MR imaging. *Radiology*, **193**, 533–538.

Ganz, T. (2007) Molecular control of iron transport. *Journal of the American Society of Nephrology*, **18**, 394–400.

Garbowski, M.W., Carpenter, J.P., Smith, G., Roughton, M., Alam, M.H., He, T., Pennell, D.J. & Porter, J.B. (2014) Biopsy-based calibration of T2* magnetic resonance for estimation of liver iron concentration and comparison with R2 Ferriscan. *Journal of Cardiovascular Magnetic Resonance*, **16**, 40.

Ghugre, N.R. & Wood, J.C. (2011) Relaxivity-iron calibration in hepatic iron overload: probing underlying biophysical mechanisms using a Monte Carlo model. *Magnetic Resonance in Medicine*, **65**, 837–847.

Ghugre, N.R., Enriquez, C.M., Gonzalez, I., Nelson, Jr, M.D., Coates, T.D. & Wood, J.C. (2006) MRI detects myocardial iron in the human heart. *Magnetic Resonance in Medicine*, **56**, 681–686.

Gianesin, B., Zefiro, D., Musso, M., Rosa, A., Bruzzone, C., Balocco, M., Carrara, P., Bacigalupo, L., Banderali, S., Rollandi, G.A., Gambaro, M., Marinelli, M. & Forni, G.L. (2012) Measurement of liver iron overload: noninvasive calibration of MRI-R2* by magnetic iron detector susceptometer. *Magnetic Resonance in Medicine*, **67**, 1782–1786.

Goldberg, H.I., Cann, C.E., Moss, A.A., Ohto, M., Brito, A. & Federle, M. (1982) Noninvasive quantitation of liver iron in dogs with hemochromatosis using dual-energy CT scanning. *Investigative Radiology*, **17**, 375–380.

Gosriwatana, I., Loreal, O., Lu, S., Brissot, P., Porter, J. & Hider, R.C. (1999) Quantification of non-transferrin-bound iron in the presence of unsaturated transferrin. *Analytic Biochemistry*, **273**, 212–220.

Hankins, J.S., McCarville, M.B., Loeffler, R.B., Smeltzer, M.P., Onciu, M., Hoffer, F.A., Li, C.S., Wang, W.C., Ware, R.E. & Hillenbrand, C.M. (2009) R2* magnetic resonance imaging of the liver in patients with iron overload. *Blood*, **113**, 4853–4855.

He, T., Smith, G.C., Gatehouse, P.D., Mohiaddin, R.H., Firmin, D.N. & Pennell, D.J. (2009) On using T2 to assess extrinsic magnetic field inhomogeneity effects on T2* measurements in myocardial siderosis in thalassemia. *Magnetic Resonance in Medicine*, **61**, 501–506.

Inati, A., Musallam, K.M., Wood, J.C. & Taher, A.T. (2010) Iron overload indices rise linearly with transfusion rate in patients with sickle cell disease. *Blood*, **115**, 2980–2981; author reply 2981-2982.

Jacobs, E.M., Hendriks, J.C., van Tits, B.L., Evans, P.J., Breuer, W., Liu, D.Y., Jansen, E.H., Jauhiainen, K., Sturm, B., Porter, J.B., Scheiber-Mojdehkar, B., von Bonsdorff, L., Cabantchik, Z.I., Hider, R.C. & Swinkels, D.W. (2005) Results of an international round robin for the quantification of serum non-transferrin-bound iron: need for defining standardization and a clinically relevant isoform. *Analytic Biochemistry*, **341**, 241–250.

Jensen, J.H. & Chandra, R. (2002) Theory of non-exponential NMR signal decay in liver with iron overload or superparamagnetic iron oxide particles. *Magnetic Resonance in Medicine*, **47**, 1131–1138.

Kattamis, A., Papassotiriou, I., Palaiologou, D., Apostolakou, F., Galani, A., Ladis, V., Sakellaropoulos, N. & Papanikolaou, G. (2006) The effects of erythropoetic activity and iron burden on hepcidin expression in patients with thalassemia major. *Haematologica*, **91**, 809–812.

Kautz, L., Jung, G., Valore, E.V., Rivella, S., Nemeth, E. & Ganz, T. (2014) Identification of erythroferrone as an erythroid regulator of iron metabolism. *Nature Genetics*, **46**, 678–684.

Kim, D., Jensen, J.H., Wu, E.X., Feng, L., Au, W.Y., Cheung, J.S., Ha, S.Y., Sheth, S.S. & Brittenham, G.M. (2011) Rapid monitoring of iron-chelating therapy in thalassemia major by a new cardiovascular MR measure: the reduced transverse relaxation rate. *NMR in Biomedicine*, **24**, 771–777.

Kirk, P., Roughton, M., Porter, J.B., Walker, J.M., Tanner, M.A., Patel, J., Wu, D., Taylor, J., Westwood, M.A., Anderson, L.J. & Pennell, D.J. (2009) Cardiac T2* magnetic resonance for prediction of cardiac complications in thalassemia major. *Circulation*, **120**, 1961–1968.

Kountouras, D., Tsagarakis, N.J., Fatourou, E., Dalagiorgos, E., Chrysanthos, N., Berdoussi, H., Vgontza, N., Karagiorga, M., Lagiandreou, A., Kaligeros, K., Voskaridou, E., Roussou, P., Diamanti-Kandarakis, E. & Koskinas, J. (2013) Liver disease in adult transfusion-dependent beta-thalassaemic patients: investigating the role of iron overload and chronic HCV infection. *Liver International*, **33**, 420–427.

Kowdley, K.V., Belt, P., Wilson, L.A., Yeh, M.M., Neuschwander-Tetri, B.A., Chalasani, N., Sanyal, A.J. & Nelson, J.E. (2012) Serum ferritin is an independent predictor of histologic severity and advanced fibrosis in patients with nonalcoholic fatty liver disease. *Hepatology*, **55**, 77–85.

Meloni, A., Rienhoff, Jr, H.Y., Jones, A., Pepe, A., Lombardi, M. & Wood, J.C. (2013) The use of appropriate calibration curves corrects for systematic differences in liver R2* values measured using different software packages. *British Journal of Hematology*, **161**, 888–891.

Meloni, A., Puliyel, M., Pepe, A., Berdoukas, V., Coates, T.D. & Wood, J.C. (2014) Cardiac iron overload in sickle-cell disease. *American Journal of Hematology*, **89**, 678–683.

Modell, B., Khan, M. & Darlison, M. (2000) Survival in beta-thalassaemia major in the UK: data from the UK Thalassaemia Register. *Lancet*, **355**, 2051–2052.

Morgan, E.H. & Walters, M.N. (1963) Iron storage in human disease: fractionation of hepatic and splenic iron into ferritin and haemosiderin with histochemical correlations. *Journal of Clinical Pathology*, **16**, 101–107.

Musallam, K.M., Cappellini, M.D., Wood, J.C., Motta, I., Graziadei, G., Tamim, H. & Taher, A.T. (2011) Elevated liver iron concentration is a marker of increased morbidity in patients with beta thalassemia intermedia. *Haematologica*, **96**, 1605–1612.

Nielsen, P., Engelhardt, R., Duerken, M., Janka, G.E. & Fischer, R. (2000) Using SQUID biomagnetic liver susceptometry in the treatment of thalassemia and other iron loading diseases. *Transfusion Sciences*, **23**, 257–258.

Noetzli, L.J., Carson, S.M., Nord, A.S., Coates, T.D. & Wood, J.C. (2008) Longitudinal analysis of heart and liver iron in thalassemia major. *Blood*, **112**, 2973–2978.

Noetzli, L.J., Papudesi, J., Coates, T.D. & Wood, J.C. (2009) Pancreatic iron loading predicts car-

diac iron loading in thalassemia major. *Blood*, **114**, 4021–4026.

Noetzli, L.J., Panigrahy, A., Mittelman, S.D., Hyderi, A., Dongelyan, A., Coates, T.D. & Wood, J.C. (2012a) Pituitary iron and volume predict hypogonadism in transfusional iron overload. *American Journal of Hematology*, **87**, 167–171.

Noetzli, L.J., Mittelman, S.D., Watanabe, R.M., Coates, T.D. & Wood, J.C. (2012b) Pancreatic iron and glucose dysregulation in thalassemia major. *American Journal of Hematology*, **87**, 155–160.

Noetzli, L.J., Panigrahy, A., Hyderi, A., Dongelyan, A., Coates, T.D. & Wood, J.C. (2012c) Pituitary iron and volume imaging in healthy controls. *AJNR. American Journal of Neuroradiology*, **33**, 259–265.

Olivieri, N.F., Nathan, D.G., MacMillan, J.H., Wayne, A.S., Liu, P.P., McGee, A., Martin, M., Koren, G. & Cohen, A.R. (1994) Survival in medically treated patients with homozygous beta-thalassemia. *New England Journal of Medicine*, **331**, 574–578.

Oudit, G.Y., Trivieri, M.G., Khaper, N., Liu, P.P. & Backx, P.H. (2006) Role of L-type Ca^{2+} channels in iron transport and iron-overload cardiomyopathy. *Journal of Molecular Medicine*, **84**, 349–364.

Pennell, D.J., Berdoukas, V., Karagiorga, M., Ladis, V., Piga, A., Aessopos, A., Gotsis, E.D., Tanner, M.A., Smith, G.C., Westwood, M.A., Wonke, B. & Galanello, R. (2006) Randomized controlled trial of deferiprone or deferoxamine in beta-thalassemia major patients with asymptomatic myocardial siderosis. *Blood*, **107**, 3738–3744.

Pennell, D.J., Porter, J.B., Cappellini, M.D., El-Beshlawy, A., Chan, L.L., Aydinok, Y., Elalfy, M.S., Sutcharitchan, P., Li, C.K., Ibrahim, H., Viprakasit, V., Kattamis, A., Smith, G., Habr, D., Domokos, G., Roubert, B. & Taher, A. (2010) Efficacy of deferasirox in reducing and preventing cardiac iron overload in beta-thalassemia. *Blood*, **115**, 2364–2371.

Pennell, D.J., Udelson, J.E., Arai, A.E., Bozkurt, B., Cohen, A.R., Galanello, R., Hoffman, T.M., Kiernan, M.S., Lerakis, S., Piga, A., Porter, J.B., Walker, J.M. & Wood, J. (2013) Cardiovascular function and treatment in beta-thalassemia major: a consensus statement from the American Heart Association. *Circulation*, **128**, 281–308.

Pfeifer, C.D., Schoennagel, B.P., Grosse, R., Wang, Z.J., Graessner, J., Nielsen, P., Adam, G., Fischer, R. & Yamamura, J. (2014) Pancreatic iron and fat assessment by MRI-R2* in patients with iron overload diseases. *Journal of Magnetic Resonance Imaging*, doi:10.1002/jmri.24752 Epub ahead of print.

Piga, A., Longo, F., Duca, L., Roggero, S., Vinciguerra, T., Calabrese, R., Hershko, C. & Cappellini, M.D. (2009) High nontransferrin bound iron levels and heart disease in thalassemia major. *American Journal of Hematology*, **84**, 29–33.

Pootrakul, P., Breuer, W., Sametband, M., Sirankapracha, P., Hershko, C. & Cabantchik, Z.I. (2004) Labile plasma iron (LPI) as an indicator of chelatable plasma redox activity in iron-overloaded beta-thalassemia/HbE patients treated with an oral chelator. *Blood*, **104**, 1504–1510.

Porter, J.B. (2007) Concepts and goals in the management of transfusional iron overload. *American Journal of Hematology*, **82**, 1136–1139.

Porter, J.B., Abeysinghe, R.D., Marshall, L., Hider, R.C. & Singh, S. (1996) Kinetics of removal and reappearance of non-transferrin-bound plasma iron with deferoxamine therapy. *Blood*, **88**, 705–713.

Porter, J.B., Walter, P.B., Neumayr, L.D., Evans, P., Bansal, S., Garbowski, M., Weyhmiller, M.G., Harmatz, P.R., Wood, J.C., Miller, J.L., Byrnes, C., Weiss, G., Seifert, M., Grosse, R., Grabowski, D., Schmidt, A., Fischer, R., Nielsen, P., Niemeyer, C. & Vichinsky, E. (2014) Mechanisms of plasma non-transferrin bound iron generation: insights from comparing transfused diamond blackfan anaemia with sickle cell and thalassaemia patients. *British Journal of Haematology*, **167**, 692–696.

Puliyel, M., Sposto, R., Berdoukas, V.A., Hofstra, T.C., Nord, A., Carson, S., Wood, J. & Coates, T.D. (2014) Ferritin trends do not predict changes in total body iron in patients with transfusional iron overload. *American Journal of Hematology*, **89**, 391–394.

Restaino, G., Meloni, A., Positano, V., Missere, M., Rossi, G., Calandriello, L., Keilberg, P., Mattioni, O., Maggio, A., Lombardi, M., Sallustio, G. & Pepe, A. (2011) Regional and global pancreatic T*2 MRI for iron overload assessment in a large cohort of healthy subjects: normal values and correlation with age and gender. *Magnetic Resonance in Medicine*, **65**, 764–769.

Roghi, A., Cappellini, M.D., Wood, J.C., Musallam, K.M., Patrizia, P., Fasulo, M.R., Cesaretti, C. & Taher, A.T. (2010) Absence of cardiac siderosis despite hepatic iron overload in Italian patients with thalassemia intermedia: an MRI T2* study. *Annals of Hematology*, **89**, 585–589.

Rose, C., Vandevenne, P., Bourgeois, E., Cambier, N. & Ernst, O. (2006) Liver iron content assessment by routine and simple magnetic resonance imaging procedure in highly transfused patients. *European Journal of Hematology*, **77**, 145–149.

Ruccione, K.S., Mudambi, K., Sposto, R., Fridey, J., Ghazarossian, S. & Freyer, D.R. (2012) Association of projected transfusional iron burden with treatment intensity in childhood cancer survivors. *Pediatric Blood & Cancer*, **59**, 697–702.

Sado, D.M., Maestrini, V., Piechnik, S.K., Banypersad, S.M., White, S.K., Flett, A.S., Robson, M.D., Neubauer, S., Ariti, C., Arai, A., Kellman, P., Yamamura, J., Schoennagel, B.P., Shah, F., Davis, B., Trompeter, S., Walker, M., Porter, J. & Moon, J.C. (2014) Noncontrast myocardial T mapping using cardiovascular magnetic resonance for iron overload. *Journal of Magnetic Resonance Imaging*, doi: 10.1002/jmri.24727.

Sohn, Y.S., Ghoti, H., Breuer, W., Rachmilewitz, E., Attar, S., Weiss, G. & Cabantchik, Z.I. (2012) The role of endocytic pathways in cellular uptake of plasma non-transferrin iron. *Haematologica*, **97**, 670–678.

St Pierre, T.G., Clark, P.R., Chua-anusorn, W., Fleming, A.J., Jeffrey, G.P., Olynyk, J.K., Pootrakul, P., Robins, E. & Lindeman, R. (2005) Noninvasive measurement and imaging of liver iron concentrations using proton magnetic resonance. *Blood*, **105**, 855–861.

St Pierre, T.G., El-Beshlawy, A., Elalfy, M., Al Jefri, A., Al Zir, K., Daar, S., Habr, D., Kriemler-Krahn, U. & Taher, A. (2014) Multicenter validation of spin-density projection-assisted R2-MRI for the noninvasive measurement of liver iron concentration. *Magnetic Resonance in Medicine*, **71**, 2215–2223.

Stark, D.D., Bass, N.M., Moss, A.A., Bacon, B.R., McKerrow, J.H., Cann, C.E., Brito, A. & Goldberg, H.I. (1983) Nuclear magnetic resonance imaging of experimentally induced liver disease. *Radiology*, **148**, 743–751.

Storey, P., Thompson, A.A., Carqueville, C.L., Wood, J.C., de Freitas, R.A. & Rigsby, C.K. (2007) R2* imaging of transfusional iron burden at 3T and comparison with 1.5T. *Journal of Magnetic Resonance Imaging*, **25**, 540–547.

Taher, A.T., Porter, J.B., Viprakasit, V., Kattamis, A., Chuncharunee, S., Sutcharitchan, P., Siritanaratkul, N., Origa, R., Karakas, Z., Habr, D., Zhu, Z. & Cappellini, M.D. (2015) Defining serum ferritin thresholds to predict clinically relevant liver iron concentrations for guiding deferasirox therapy when MRI is unavailable in patients with non-transfusion-dependent thalassaemia. *British Journal of Hematology*, **168**, 284–90.

Tanner, M.A., He, T., Westwood, M.A., Firmin, D.N. & Pennell, D.J. (2006) Multi-center validation of the transferability of the magnetic resonance T2* technique for the quantification of tissue iron. *Haematologica*, **91**, 1388–1391.

Tanner, M.A., Galanello, R., Dessi, C., Smith, G.C., Westwood, M.A., Agus, A., Roughton, M., Assomull, R., Nair, S.V., Walker, J.M. & Pennell, D.J. (2007) A randomized, placebo-controlled, double-blind trial of the effect of combined therapy with deferoxamine and deferiprone on myocardial iron in thalassemia major using cardiovascular magnetic resonance. *Circulation*, **115**, 1876–1884.

Tanner, M.A., Galanello, R., Dessi, C., Smith, G.C., Westwood, M.A., Agus, A., Pibiri, M., Nair, S.V., Walker, J.M. & Pennell, D.J. (2008) Combined chelation therapy in thalassemia major for the treatment of severe myocardial siderosis with left ventricular dysfunction. *Journal of Cardiovascular Magnetic Resonance*, **10**, 12.

Tsai, Y.S., Chen, J.S., Wang, C.K., Lu, C.H., Cheng, C.N., Kuo, C.S., Liu, Y.S. & Tsai, H.M. (2014) Quantitative assessment of iron in heart and liver phantoms using dual-energy computed tomography. *Experimental Therapeutics in Medicine*, **8**, 907–912.

Villeneuve, J.P., Bilodeau, M., Lepage, R., Cote, J. & Lefebvre, M. (1996) Variability in hepatic iron

concentration measurement from needle-biopsy specimens. *Journal of Hepatology*, **25**, 172–177.

Wali, Y.A., Taqi, A. & Deghaidi, A. (2004) Study of intermittent intravenous deferrioxamine high-dose therapy in heavily iron-loaded children with beta-thalassemia major poorly compliant to subcutaneous injections. *Pediatric Hematology Oncology*, **21**, 453–460.

Walter, P.B., Fung, E.B., Killilea, D.W., Jiang, Q., Hudes, M., Madden, J., Porter, J., Evans, P., Vichinsky, E. & Harmatz, P. (2006) Oxidative stress and inflammation in iron-overloaded patients with beta-thalassaemia or sickle cell disease. *British Journal of Hematology*, **135**, 254–263.

Westwood, M.A., Anderson, L.J., Firmin, D.N., Gatehouse, P.D., Lorenz, C.H., Wonke, B. & Pennell, D.J. (2003) Interscanner reproducibility of cardiovascular magnetic resonance T2* measurements of tissue iron in thalassemia. *Journal of Magnetic Resonance Imaging*, **18**, 616–620.

Westwood, M.A., Anderson, L.J., Maceira, A.M., Shah, F.T., Prescott, E., Porter, J.B., Wonke, B., Walker, J.M. & Pennell, D.J. (2007) Normalized left ventricular volumes and function in thalassemia major patients with normal myocardial iron. *Journal of Magnetic Resonance Imaging*, **25**, 1147–1151.

Wood, J.C. (2008) Cardiac iron across different transfusion-dependent diseases. *Blood Reviews*, **22**, S14–S21.

Wood, J.C. (2009) History and current impact of cardiac magnetic resonance imaging on the management of iron overload. *Circulation*, **120**, 1937–1939.

Wood, J.C. (2014) Use of magnetic resonance imaging to monitor iron overload. *Hematology Oncology Clinics of North America*, **28**, 747–764, vii.

Wood, J.C., Enriquez, C., Ghugre, N., Tyzka, J.M., Carson, S., Nelson, M.D. & Coates, T.D. (2005a) MRI R2 and R2* mapping accurately estimates hepatic iron concentration in transfusion-dependent thalassemia and sickle cell disease patients. *Blood*, **106**, 1460–1465.

Wood, J.C., Enriquez, C., Ghugre, N., Otto-Duessel, M., Aguilar, M., Nelson, M.D., Moats, R. & Coates, T.D. (2005b) Physiology and pathophysiology of iron cardiomyopathy in thalassemia. *Annals of the New York Academy of Sciences*, **1054**, 386–395.

Wood, J.C., Otto-Duessel, M., Aguilar, M., Nick, H., Nelson, M.D., Coates, T.D., Pollack, H. & Moats, R. (2005c) Cardiac iron determines cardiac T2*, T2, and T1 in the gerbil model of iron cardiomyopathy. *Circulation*, **112**, 535–543.

Wood, J.C., Kang, B.P., Thompson, A., Giardina, P., Harmatz, P., Glynos, T., Paley, C. & Coates, T.D. (2010) The effect of deferasirox on cardiac iron in thalassemia major: impact of total body iron stores. *Blood*, **116**, 537–543.

Wood, J.C., Glynos, T., Thompson, A., Giardina, P., Harmatz, P., Kang, B.P., Paley, C. & Coates, T.D. (2011a) Relationship between labile plasma iron, liver iron concentration and cardiac response in a deferasirox monotherapy trial. *Haematologica*, **96**, 1055–1058.

Wood, J.C., Mo, A., Gera, A., Koh, M., Coates, T. & Gilsanz, V. (2011b) Quantitative computed tomography assessment of transfusional iron overload. *British Journal of Hematology*, **153**, 780–785.

Wood, J.C., Zhang, P., Rienhoff, H., Abi-Saab, W. & Neufeld, E. (2013) Liver MRI is better than biopsy for assessing total boday iron balance: validation by simulation. *Blood*, **122**, 958.

Wood, J.C., Zhang, P., Rienhoff, H., Abi-Saab, W. & Neufeld, E. (2014) R2 and R2* are equally effective in evaluating chronic response to iron chelation. *American Journal of Hematology*, **89**, 505–508.

Zanninelli, G., Breuer, W. & Cabantchik, Z.I. (2009) Daily labile plasma iron as an indicator of chelator activity in thalassaemia major patients. *British Journal of Hematology*, **147**, 744–751.